Strong Field Interactions between a Nanomagnet and a Photonic Cavity

Ö. O. Soykal and M. E. Flatté

Optical Science and Technology Center and Department of Physics and Astronomy, University of Iowa, Iowa City, Iowa 52242, USA

(Received 15 July 2009; published 18 February 2010)

We analyze the interaction of a nanomagnet (ferromagnetic) with a single photonic mode of a cavity in a fully quantum-mechanical treatment and find that exceptionally large quantum-coherent magnet-photon coupling can be achieved. Coupling terms in excess of several THz are predicted to be achievable in a spherical cavity of ~1 mm radius with a nanomagnet of ~100 nm radius and ferromagnetic resonance frequency of ~200 GHz. Eigenstates of the magnet-photon system correspond to entangled states of spin orientation and photon number, in which over 10^5 values of each quantum number are represented; conversely, initial (coherent) states of definite spin and photon number evolve dynamically to produce large oscillations in the microwave power (and nanomagnet spin orientation), and are characterized by exceptionally long dephasing times.

DOI: 10.1103/PhysRevLett.104.077202 PACS numbers: 75.75.−c, 85.75.−d

Strong coupling between light and electronic transitions [1–7] permits coherent transfer of quantum information between the two systems, as well as a host of exotic phenomena, including slow light [8,9], lasing without population inversion [10,11], and index enhancement via quantum coherence [12,13]. Achieving strong coupling between light and electronic transitions in solids has been challenging, due to the shorter coherence time of electrical dipole transitions in solids compared to atoms; however, strong coupling in a single quantum dot-semiconductor microcavity system [14] has been demonstrated with a coupling strength ~80 μeV. Often these investigations in solids focus on electric dipole (orbital) transitions over magnetic (spin) transitions, whose typical oscillator strengths are estimated [15] to be smaller by a factor of the fine structure constant, ~1/137. Paramagnetic spin systems in solids, however, appear intrinsically more quantum coherent than orbital coherent states [16,17], and collective spin-photon effects (such as superradiance [18,19], including in molecular magnets of ~10 spins [20]) are known. Yet to be explored are the coherent strong-field properties of ferromagnetic systems. In ferromagnets, the exchange interaction can cause a very large number of spins to lock together into one macrospin with a corresponding increase in oscillator strength. Therefore, for nanomagnets with ~100 spins or more, the electronic-photonic coupling strength may exceed that of a two-level electronic orbital transition occurring by electric dipole coupling, while still maintaining long coherence times (ferromagnetic nanomagnet oscillators have been demonstrated [21,22] with Q factors in excess of 500). Such ferromagnetic oscillations can be coherently driven by electrical spin currents [22–27], and thus a single nanomagnet-photonic mode system provides an efficient method of strongly coupling electronic, magnetic and photonic degrees of freedom.

Here, we calculate the strong-field interactions between a small ferromagnet (nanomagnet) and light, and find a dramatic enhancement of spin-photon coupling relative to paramagnetic spin systems, yielding coupling much larger than found by coupling light to orbital transitions. As shown schematically in Fig. 1, the oscillator is a spherical nanomagnet with a radius r_m possessing a very large spin $\boldsymbol{S}$. This spin, arising from an assembly of N electron spins (for $r_m \sim 100$ nm, $N \sim 10^9$) exchange locked in parallel, can be treated as a macrospin. This nanomagnet is placed a distance d from the center of the cavity for more efficient coupling to the cavity mode. High frequency precession of the nanomagnet at a frequency resonant with the cavity is achieved by tuning a uniform magnetic field $\boldsymbol{B}_0$ along the $\mathbf{z}$ axis of the cavity. We find for a realistic cavity size (~1 mm) and resonance frequency (~200 GHz) that photonic coupling terms between neighboring spin states when the cavity is empty of photons are comparable in size to those of quantum dot electric dipole transitions (~100 μeV) [14]. This spin-photon coupling leads to ei-

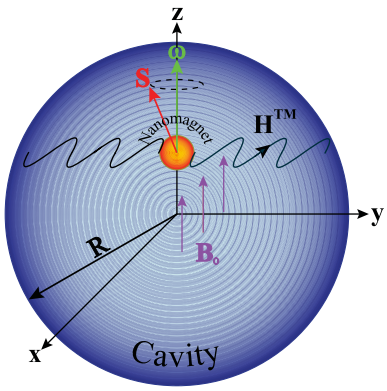

FIG. 1 (color). Schematic of the nanomagnet-cavity system with a spherical nanomagnet of radius r_m placed at a distance of d from the center of a cavity of radius R. A uniform magnetic field, $\boldsymbol{B}_0$, applied along the $\mathbf{z}$ axis causes precession of the nanomagnet macrospin, $\boldsymbol{S}$, with frequency of ω, in resonance with TM mode of the cavity.

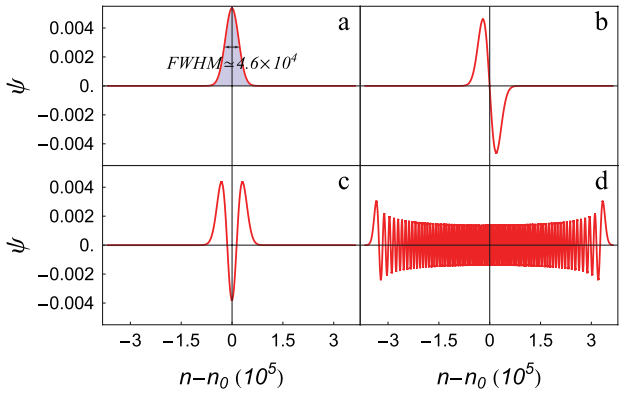

FIG. 2 (color). Wave functions of the nanomagnet-cavity system as a function of photon number, n, centered about $n_0 = 4\xi/3 = 6.666\,67 \times 10^8$ for $N = 10^9$ spins: (a) ground state with a width of roughly 5×10^4 photons (or equivalently spin quantum numbers m_s), (b) 1st, (c) 2nd, and (d) 150th excited states.

genstates of the mixed system which extend over 10^5 values of spin and photon quantum numbers, as shown in Fig. 2. We also find an unexpected regime, in which the system is initialized with (1) no photons and (1) the nanomagnet in its high-energy (antiparallel) orientation to the magnetic field, whereby large oscillations in spin number and photon number result (Fig. 3), corresponding to spin-photon coupling strengths between neighboring spins ~160 meV (~40 THz). These large oscillations in spin and photon number (~10^5 quanta of each) on μs time scales are characterized by long dephasing times (Fig. 4).

The total Hamiltonian of the system incorporates the magnetic $\boldsymbol{H}$ and electric fields $\boldsymbol{E}$ of the cavity and the magnetization $\boldsymbol{M}$ of the nanomagnet [15],

$$\mathcal{H} = \frac{1}{2}\int [\mu_0|\boldsymbol{H}|^2 + \epsilon_0|\boldsymbol{E}|^2 + \mu_0(\boldsymbol{H}\cdot\boldsymbol{M})]d^3r. \quad (1)$$

The first two integrands on the right-hand side of Eq. (1) correspond to the free field Hamiltonian, whereas the third integrand describes the interaction Hamiltonian of the nanomagnet-cavity system. Spherical wave expansion of the cavity field [28] and renormalization of the field strength coefficients to satisfy $[a_{lm}, a^\dagger_{l'm'}] = \delta_{ll'}\delta_{mm'}$ yield the interaction Hamiltonian

$$\mathcal{H}_I = \Big[\sum_{l,m}\Gamma_l^{(\mathrm{TE})} a_{lm}^{(\mathrm{TE})}\int_S \boldsymbol{M}\cdot(\boldsymbol{\nabla}\times\boldsymbol{u}_{lm})d^3r + \sum_{l,m}\Gamma_l^{(\mathrm{TM})} a_{lm}^{(\mathrm{TM})}\int_S \boldsymbol{M}\cdot\boldsymbol{u}_{lm}d^3r\Big] + \mathrm{H.c.} \quad (2)$$

where the basis functions for spherical waves are given by $\boldsymbol{u}_{lm}$. Moreover, the coupling constants for transverse electric, and transverse magnetic modes of the field for angular momentum l are $\Gamma_l^{(\mathrm{TE})}$ and $\Gamma_l^{(\mathrm{TM})}$, respectively.

A nanomagnet acting as a macrospin, as seen experimentally in nanomagnet oscillators of roughly this size [22], has a magnetization $\boldsymbol{M} = \boldsymbol{\mu}/V = -\boldsymbol{S}(g_s\mu_B/\hbar V) \times$

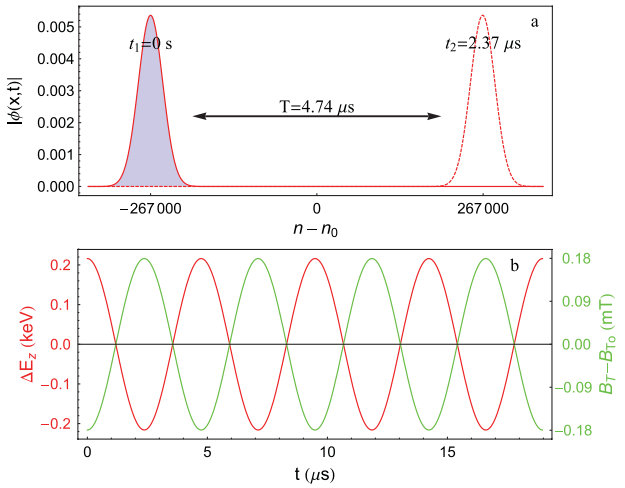

FIG. 3 (color). (a) Amplitude of a coherent state of nanomagnet/photon system shown as a function of photon number n. The large oscillations of this coherent state about $n_0 = 6.667 \times 10^8$ occur between photon numbers $-267\,000$ (*Filled line*), and $+267\,000$ (*Dashed line*) with a period of $T = 4.74$ μs. (b) Time evolution of the Zeeman energy of the nanomagnet (*Red line*), and transverse magnetic mode of the cavity field (*Green line*) at $z = d$ in this coherent state representation.

$\Theta(r_m - |\boldsymbol{r} - \boldsymbol{d}|)$, where $\Theta(x)$ is the Heaviside step function. As one example, a spherical nanomagnet of iron, radius $r_m \cong 108$ nm, corresponds to 10^9 iron spins exchange locked in parallel.

For the spherical wave expansion of the magnetic field, all components of the field vanish if $l = m = 0$ (no radiating monopoles). For a magnetic field applied in the $\hat{z}$ direction, the microwave emission of the nanomagnet is due to the oscillating components of the magnetization $\boldsymbol{M}_{x,y}$ perpendicular to the radial direction (Fig. 1), and thus the cavity TE modes (magnetic field pointing in the radial direction) do not couple to the nanomagnet. The basis functions for the lowest-frequency (dominant) dipole TM mode ($l = 1$) are given by $\boldsymbol{u}_{1m} = j_1(kr)\mathbf{Y}_{1,1,m}(\theta, \phi)$.

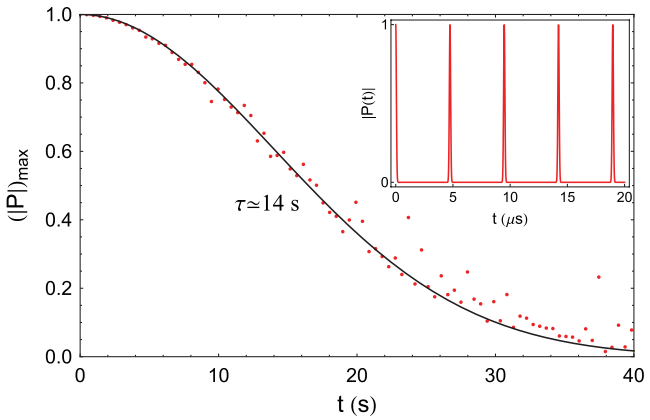

FIG. 4 (color). Dephasing time of the coherent state obtained by a Gaussian fit to the peak values of the correlation function (inset) at successive time intervals.

The vector spherical harmonic $\mathbf{Y}_{1,1,m}$ is expanded using the helicity basis vectors $\hat{\mathbf{e}}_{\mathbf{m}}$ [which form a spherical tensor of rank 1, i.e., $\hat{\mathbf{e}}_{\pm} = \mp(\hat{\mathbf{x}} \pm i\hat{\mathbf{y}})/\sqrt{2}$, $\hat{\mathbf{e}}_{\mathbf{0}} = \hat{\mathbf{z}}$]. The spin operator of the nanomagnet in the helicity basis, $\boldsymbol{S} = \frac{1}{\sqrt{2}}(S_+\hat{\mathbf{e}}_- - S_-\hat{\mathbf{e}}_+) + S_z\hat{\mathbf{e}}_0$, in terms of the spin raising and lowering operators $[S_\pm|l_s, m_s\rangle = \sqrt{(l_s \mp m_s)(l_s \pm m_s + 1)}|l_s, m_s \pm 1\rangle]$. Introduction of this total spin operator to Eq. (2), as well as replacing the field strength coefficients of the TM mode with the corresponding annihilation (creation) operators, yields a fully quantum Hamiltonian

$$\mathcal{H}_\gamma = \hbar\omega_\gamma\left(a_\gamma^\dagger a_\gamma + \frac{1}{2}\right) - g\mu_B\Gamma_\gamma(a_\gamma S_+ + a_\gamma^\dagger S_-) + g\frac{\mu_B}{\hbar}B_0 S_z, \tag{3}$$

in which the spin interacts only with a single photon mode γ. Modes of higher l would be out of resonance because of the cavity quantization, and energy nonconserving terms with negative helicity have been dropped (relying on the rotating wave approximation [29]). The nanomagnet-photon coupling constant, Γ_γ, is found to be

$$\Gamma_\gamma = \frac{j_1(kd)}{8\hbar|j_1(y_{1\gamma})|}\left[1 - \frac{l(l+1)}{y_{1\gamma}^2}\right]^{-1/2}\sqrt{\frac{3\hbar\omega_\gamma\mu_0}{\pi R^3}}, \tag{4}$$

where $y_{1\gamma}$ is the γ-th zero of $|rj_1(kr)|'$ satisfying the conditions for the field of TM mode at the cavity boundary. The mode frequency ω_γ is related to the radius of the cavity R with $k_{1\gamma} = \omega_{1\gamma}/c = y_{1\gamma}/R$. The cavity is in resonance with the energy level splitting of the spins whenever $\hbar\omega_\gamma = g\mu_B B_0$, when any spin-flip up (down) process of the nanomagnet results in an absorption (emission) of a cavity photon. An applied uniform magnetic field of $B_0 = 7$ T, corresponding to a precession of the macrospin with a frequency of $\sim$200 GHz, will cause the nanomagnet spins to be in resonance with a cavity volume of 1.25 mm^3. We assume the lowest TM mode of the cavity is in resonance with the spin-flip transitions of the nanomagnet, so as higher-energy modes will not be in resonance, the subscript γ will be dropped from Eq. (3).

The eigenstates of the nanomagnet's macrospin are simultaneous eigenstates of $\boldsymbol{S}^2$ and $\boldsymbol{S}_z$ given by $|l_s, m_s\rangle$, where $|m_s| \le l_s \le N/2$. Part of the macrospin approximation is the assumption that l_s is fixed, and we assume the maximal spin state, $l_s = N/2$. The total excitation number $\xi = n + m_s$, where n is the photon number of the nanomagnet-cavity system, is conserved by the Hamiltonian of Eq. (3). For an initial configuration of the macrospin pointing antiparallel to the static field $\boldsymbol{B}_0$ and no photons in the cavity, $\xi = N/2$, the basis states of the spin-photon mode system $|n, m_s\rangle$ can be indexed either solely by n or by m_s: $|n, \xi - n\rangle$ or $|\xi - m_s, m_s\rangle$. The structure of these basis states is similar to those of the Dicke model [1] for N independent atomic spins, wherein l_s is the *cooperation number* of the paramagnetic collection of spins. The Hilbert space of N independent spins includes the states of a macrospin corresponding to $l_s = N/2$. The assumption $\xi = N/2$ corresponds to the initially fully excited atomic system in the Dicke model, with no photons in the cavity. However, for a real nanomagnet (like in our case), elements of the Hilbert space with $l_s \neq N/2$ are split off in energy due to the exchange interaction.

To proceed, we drop the redundant reference to m_s, so $|n, \xi - n\rangle \to |n\rangle$, and

$$\mathcal{H} = \sum_{n=0}^{2\xi} E_0|n\rangle\langle n| - \tau(n)[|n+1\rangle\langle n| + |n\rangle\langle n+1|], \tag{5}$$

in the Fock space, where the constant energy coefficient E_0 term and the coupling strength $\tau(x)$ are defined as

$$E_0 = \hbar\omega(\xi + 1/2), \qquad \tau(n) = \hbar\Gamma g\mu_B(n+1)\sqrt{2\xi - n}. \tag{6}$$

For $2\xi = N$, the magnet-microwave mode coupling, $\tau(n)$, changes over a range of 0.10 MHz-4.1 THz through all possible n. $\tau(n)$ acts like a driving force for a fictitious particle moving between sites labeled by n, so $|0\rangle \to \ldots \to |n-1\rangle \to |n\rangle \to |n+1\rangle \to \ldots \to |2\xi\rangle$. The solutions n_0 of $\tau'(n)|_{n_0} = 0$ are equilibrium points in n, and there is one at $n_0 = (4\xi - 1)/3$. The coupling in terms of m_s is $\tau(m_s) = \hbar\Gamma g\mu_B(\xi - m_s + 1)\sqrt{\xi + m_s}$, with an equilibrium point of $m_0 = (1 - \xi)/3$.

For transitions from $|n, m_s\rangle$ which conserve energy and in which a photon is emitted, the rate of emission $R_n \propto \sum_{\forall\Psi}|\langle\Psi|a^\dagger S_-|n, m_s\rangle|^2$, where $|\Psi\rangle$ represents the possible final states of the system. R_n reaches its maximum value of $4A(N/3)^3$ for the equilibrium point m_0 (or n_0) in the large-spin limit; thus, n_0 and m_0 are the photon number and spin number, respectively, where the nanomagnet-cavity system exhibits *superradiance* [1].

The eigenfunctions of the nanomagnet-cavity Hamiltonian given in Eq. (5) can be expanded as $\Psi_j = \sum_{n'}^{2s_z}\psi_j^{n'}|n'\rangle$. For a large-spin nanomagnet, the eigenfunctions of the Hamiltonian can be found in the continuum limit, corresponding to replacing $\psi_j^n \to \psi_j(x = n\varepsilon)$ and keeping terms up to $\mathcal{O}(\varepsilon^3)$, yielding

$$\tau(x)\frac{d^2\psi_j(x)}{dx^2} + \frac{d\tau(x)}{dx}\frac{d\psi_j(x)}{dx} + \left(2\tau(x) - \frac{d\tau(x)}{dx} + \frac{1}{2}\frac{d^2\tau(x)}{dx^2} + E_j\right)\psi_j(x) = 0, \tag{7}$$

with $\psi_j(0) = \psi_j(2s_z) = 0$. The lowest energy eigenvalues E_j and eigenfunctions $\psi_j(x)$ of this differential equation, shown in Fig. 2, can be obtained in the WKB approximation from $S(E_j) = (1/2\pi)\oint\sqrt{[E_j - V_e(x)/\tau(x)]}dx = j + \frac{1}{2}$, where the effective potential is $V_e(x) = \tau'(x) + \tau'^2(x)/4\tau(x) - \tau'(x)/2\tau(x) - 2\tau(x)$. The ground state

$\psi(x)$ is extended over a broad range of x (and thus m_s and n) because $V_e(x)$ is smoothly varying (due to large ξ); in the limit of large S and large ξ, from the functional form of $V_e(x)$, the width of the ground state can be determined from $(\Delta n)^2/n_0 \sim 1$.

Coherent states, characterized by large oscillations in n about n_0, can be expressed $\phi(x,t) = \sum_{j=0}^{j_0} A_j e^{-iE_j t/\hbar}\psi_j(x)$, where $\phi(x, t = 0)$ is a Gaussian wave function centered at $x_0 = 6.664 \times 10^8$. Summation over the first 150 states describes a coherent state oscillating over a range of 5.34×10^5 photons with a period of $T = 4.74$ μs, as shown in Fig. 3(a). The large oscillations in Zeeman energy of the nanomagnet ($\boldsymbol{\mu} \cdot \boldsymbol{B}_0$), and in the cavity photon's magnetic field amplitude $\boldsymbol{B}_T$, shown in Fig. 3(b), emphasize the coherent nature of this state.

To explore the decoherence of this nanomagnet-photon system, we calculate the autocorrelation, $P(t) = |\langle\phi(t)|\phi(0)\rangle|^2$. Each peak (inset of Fig. 4) represents the maximal $P(t)$ after an oscillation period T. The dephasing due to the inhomogeneous $\tau(n)$ in Eq. (5) yields an exceptionally long dephasing time of roughly $\tau = 14$ s (Fig. 4); this dephasing time approaches infinity as $S \rightarrow \infty$. We have also assumed an infinite Q for the cavity; for a real cavity, the coherence of the nanomagnet will be reduced by photon leakage from the cavity. The principal effect of magnetic anisotropy will be to shift the precession frequency of the nanomagnet, which can be compensated for with a slight change in the applied magnetic field. Crystalline magnetic anisotropy of iron will produce a small detuning ($\sim 3 \times 10^{-10}$ eV) of the E_0 in Eq. (5) over the range of oscillation in Fig. 3. This detuning is much smaller than the couplings $\tau(n)$ in Eq. (5) and so will not destroy the coherent oscillations here, although it may limit the dephasing times to shorter than shown in Fig. 4. A cutoff of the dephasing times shown in Fig. 4 in real nanomagnets will occur from spin-lattice coupling (of m_s to phonons through spin-orbit coupling). For spheres of yttrium iron garnet (YIG) at low temperature, this spin-lattice time is several μs [30,31], permitting observation of a full oscillation cycle. The times at room temperature in YIG ($\sim$200 ns [30]) and iron ($\sim$20 ns [32]) are too small to observe a full oscillation; however, coherent dynamics corresponding to a portion of the oscillation involving $\sim$220 photons/ns, or $\sim$4400 photons for iron and 4.4×10^4 photons for YIG should be observable.

The strong-field interactions between a nanomagnet of radius 100 nm consisting of 10^9 spins and a spherical cavity roughly 1 mm^3 in volume in the presence of a static magnetic field of $\sim$7 T in magnitude indicate that strong-field coupling between magnets and light is possible, and should substantially exceed the coupling observed in solids between orbital transitions and light. The interaction Hamiltonian contains magnet-microwave mode coupling terms that can exceed several THz. Furthermore, the coherent states of the spin-photon coupling around the superradiance regime are characterized by large oscillations in photon number n of the cavity (or equivalently, the total spin quantum number m_s of the nanomagnet) with exceptionally long dephasing times.

This work was supported by an ONR MURI.

[1] R. H. Dicke, Phys. Rev. **93**, 99 (1954).
[2] M. Tavis and F. W. Cummings, Phys. Rev. **170**, 379 (1968).
[3] E. T. Jaynes and F. W. Cummings, Proc. IEEE **51**, 89 (1963).
[4] H. J. Kimble, Phys. Scr. **T76**, 127 (1998).
[5] J. M. Raimond, M. Brune, and S. Haroche, Rev. Mod. Phys. **73**, 565 (2001).
[6] A. Kiraz *et al.*, Appl. Phys. Lett. **78**, 3932 (2001).
[7] H. Walther, Adv. Chem. Phys. **122**, 167 (2002).
[8] K. J. Boller, A. Imamoglu, and S. E. Harris, Phys. Rev. Lett. **66**, 2593 (1991).
[9] L. V. Hau, S. E. Harris, Z. Dutton, and C. H. Behroozi, Nature (London) **397**, 594 (1999).
[10] M. O. Scully and M. Fleischhauer, Science **263**, 337 (1994).
[11] G. G. Padmabandu *et al.*, Phys. Rev. Lett. **76**, 2053 (1996).
[12] O. Kocharovskaya, P. Mandel, and M. O. Scully, Phys. Rev. Lett. **74**, 2451 (1995).
[13] S. Sultana and M. S. Zubairy, Phys. Rev. A **49**, 438 (1994).
[14] A. Forchel *et al.*, Nature (London) **432**, 197 (2004).
[15] J. D. Jackson, *Classical Electrodynamics* (Wiley, New York, 1998), 3rd ed., p. 259.
[16] D. D. Awschalom, N. Samarth, and D. Loss, *Semiconductor Spintronics and Quantum Computation* (Springer Verlag, Heidelberg, 2002).
[17] D. D. Awschalom and M. E. Flatté, Nature Phys. **3**, 153 (2007).
[18] G. Feher, J. P. Gordon, E. Buehler, E. A. Gere, and C. D. Thurmond, Phys. Rev. **109**, 221 (1958).
[19] M. G. Benedict, *Super-Radiance: Multiatomic Coherent Radiation* (CRC Press, New York, 1996).
[20] E. M. Chudnovsky and D. A. Garanin, Phys. Rev. Lett. **89**, 157201 (2002); V. I. Yukalov Laser Phys. **12**, 1089 (2002).
[21] W. H. Rippard *et al.*, Phys. Rev. Lett. **92**, 027201 (2004).
[22] J. C. Sankey *et al.*, Phys. Rev. Lett. **96**, 227601 (2006).
[23] L. Berger, Phys. Rev. B **54**, 9353 (1996).
[24] J. Slonczewski, J. Magn. Magn. Mater. **159**, L1 (1996).
[25] E. B. Myers *et al.*, Science **285**, 867 (1999).
[26] S. I. Kiselev *et al.*, Nature (London) **425**, 380 (2003).
[27] S. Urazhdin *et al.*, J. Appl. Phys. **97**, 10C701 (2005).
[28] W. Heitler, *The Quantum Theory of Radiation* (Dover, New York, 1998), 3rd ed., p. 402.
[29] M. O. Scully and M. S. Zubairy, *Quantum Optics* (Cambridge, Cambridge, 1997).
[30] R. C. LeCraw and E. G. Spencer, J. Phys. Soc. Jpn. **17**, 401 (1962), Supp. B1.
[31] M. Sparks and C. Kittel, Phys. Rev. Lett. **4**, 232 (1960).
[32] Z. Frait and D. Fraitova, J. Magn. Magn. Mater. **15–18**, 1081 (1980).